Communication

Homochiral Covalent Organic Framework for Catalytic Asymmetric Synthesis of Drug Intermediate

Hui-Chao Ma, Gong-Jun Chen, Fang Huang, and Yu-Bin Dong

J. Am. Chem. Soc., **Just Accepted Manuscript** • DOI: 10.1021/jacs.0c04722 • Publication Date (Web): 23 Jun 2020

Homochiral Covalent Organic Framework for Catalytic Asymmetric Synthesis of Drug Intermediate

Hui-Chao Ma, Gong-Jun Chen,* Fang Huang, and Yu-Bin Dong*

College of Chemistry, Chemical Engineering and Materials Science, Collaborative Innovation Center of Functionalized Probes for Chemical Imaging in Universities of Shandong, Key Laboratory of Molecular and Nano Probes, Ministry of Education, Shandong Normal University, Jinan 250014, P. R. China.

ABSTRACT: (*S*)-2-(2-Chlorophenyl)-2-(6,7-dihydrothieno[3,2-c]pyridin-5(4H)-yl)acetonitrile (**(*S*)-CIK**) is a key intermediate to (*S*)-clopidogrel which is one of the most saleable worldwide antiplatelet and antithrombotic drugs. We show herein a facile method for direct synthesis of **(*S*)-CIK** via Strecker reaction using homochiral covalent framework catalyst in a heterogeneous way. The asymmetric synthesis involves a photothermal conversion triggered thermally-driven reaction which affords **(*S*)-CIK** in 98% yield with 94% enantiomeric excess under visible-light irradiation. Furthermore, the above approach is readily extended to a gram-scale level on a fixed-bed continuous-flow model reactor. The potential utility of this strategy is highlighted by the preparation of many more other types of chiral drugs and drug intermediates in a green and facile way.

Chiral drugs are closely related to our health. For example, the famous thalidomide tragedy[1] allows us to fully realize that the enantiomeric composition of chiral drugs is life-critical because the biological targets are usually chiral.[2,3] In comparison to racemate resolution and chiral induction, asymmetric catalysis has been recognized as the most efficient approach to access chiral drugs and drug intermediates.[4]

Clopidogrel,[5] as an important antiplatelet and antithrombotic drug, its (*S*)-isomer is widely used to reduce the stroke risk, blood clot, and serious heart problem. (*S*)-clopidogrel bisulfate is now sold in 110 countries and has been become one of the worldwide top-selling drugs.[5-7] Instead of antithrombotic function, its (*R*)-isomer can cause social turmoil as revealed by the animal experiments.[8]

As reported, one of the most efficient approaches for synthesis of (*S*)-clopidogrel is to proceed through a **(*S*)-CIK** intermediate which can be readily transformed to (*S*)-clopidogrel via subsequent alkaline hydrolysis and salt formation steps.[5,9] The existing methods for **(*S*)-CIK** synthesis, however, usually suffer from high time, energy and resource consumption, and tedious workup.[5] For example, it can be obtained in 92% yield with an enantiomeric ratio of 78:22, but the reaction was conducted at -20°C with chiral molecular hydroquinone catalyst and NaF auxiliary in 16h in a homogeneous way.[9] Therefore, the development of step-economical and environmentally benign **(*S*)-CIK** synthetic methodology, especially for pharmaceutical industry,[10] is highly imperative.

Since the pioneering work of Yaghi in 2005,[11] covalent organic frameworks (COFs) have drawn more and more attention due to their versatile potential applications. For instance, several recent reports revealed that the homochiral covalent organic frameworks (HCCOFs)-based catalysts can elegantly promote asymmetric organic transformations in heterogeneous way.[12]

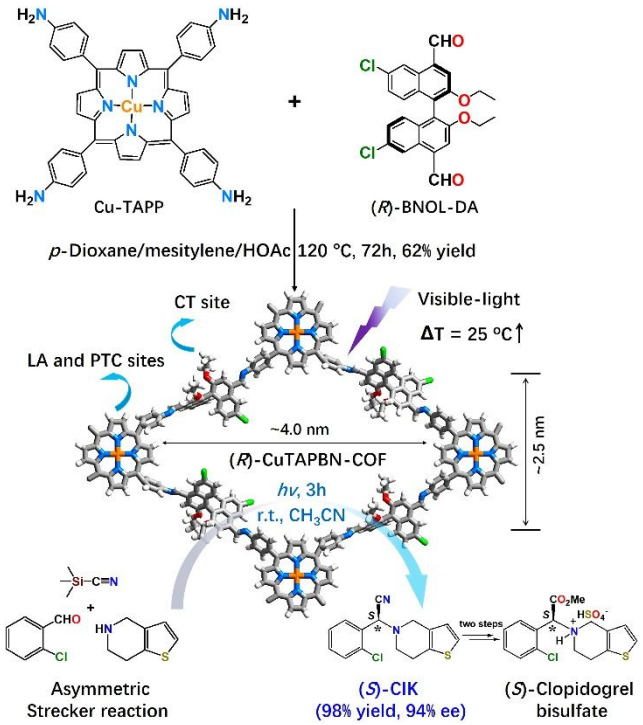

Figure 1. Synthesis and crystal structure of **(*R*)-CuTAPBN-COF**, and diagram representation of catalytic synthesis of **(*S*)-CIK**.

For meeting the multifaceted requirements of **(*S*)-CIK** synthesis with a facile single-step operation, a 5,10,15,20-tetrakis-(4-aminophenyl)-porphyrin-Cu-(II) (Cu-TAPP) and 6,6'-dichloro-2,2'-diethoxy-1,1'-binaphthyl-4,4'-dialdehyde ((*R*)-BINOL-DA) derived HCCOF, which possesses Lewis acid (LA), chiral templating (CT) and photothermal conversion (PTC) species, was designed and prepared (Figure 1, Supporting Information). Upon visible-light irradiation, the obtained **(*R*)-CuTAPBN-COF** displays excellent catalytic

activity and enantioselectivity for the **(*S*)-CIK** synthesis via asymmetric Strecker reaction (Figure 1).[13, 14]

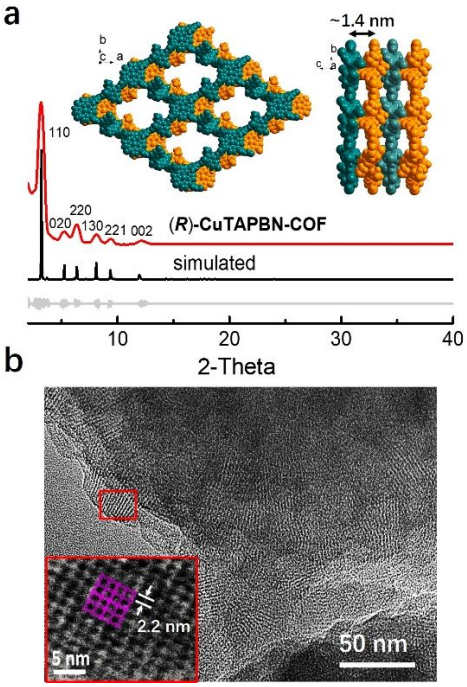

Figure 2. (a) Simulated and measured PXRD patterns of **(*R*)-CuTAPBN-COF**. Its crystal structure (top and side views) is shown as insets. (b) HR-TEM images of **(*R*)-CuTAPBN-COF** with the region marked by the red square at a higher resolution.

Scanning electron microscopy (SEM) was used to visualize the as-synthesized **(*R*)-CuTAPBN-COF**, and its particle morphology was observed (Figure S1a). Thermogravimetric analysis (TGA) indicated that **(*R*)-CuTAPBN-COF** remained intact till temperature over 250°C (Figure S1b). In addition, the existence of imine-connected Cu-TAPP and (*R*)-BINOL in **(*R*)-CuTAPBN-COF** were directly evidenced by the IR (Figure S1c) and ^{13}C CP-MAS (Figure S1d) spectra.

The crystal structure of **(*R*)-CuTAPBN-COF** was elucidated using PXRD (Figure 2a) by Materials Studio software (ver. 2018). The most probable structure was established, analogous to that of HCCOF as a 2D staggered layered-sheets using the chiral space group of *C*2 with the optimized parameters of a = 49.52, b = 33.72 and c = 15.30 Å; $\alpha = \gamma = 90°$, $\beta = 104.5°$ (residuals *R*wp = 2.15% and *R*p = 3.03%, Table S1). The first intense peak in the PXRD pattern at 3.2° (2θ), which corresponds to the (110) reflection plane, along with a series of weak peaks at 5.3°, 6.4°, 8.1°, 9.4° and 11.9°, attributed to the (020), (220), (130), (221) and (002) reflection planes, respectively. The difference plot indicates that PXRD obtained through Pawley refinement well reproduces the experimental pattern (Figure 2a). The structural modeling shows that the Cu-TAPP is linked together via (*R*)-BINOL into a 2D net extended in the crystallographic *ab* plane with rhombus-like pore, in which the shortest opposite C···C distances are ~2.5 and 4.0 nm, respectively (Figure 1). These nets are further linked together via interlayer Cl···H-C ($d_{C\text{-}H}$ = 1.914 Å, ∠Cl···H-C = 131.99°) bonds (Figure S1e) into an AB-stacking model to form the slightly reduced channels (~2.2 nm) along the crystallographic *c* axis. A long interlayer Cu···Cu distance of ~1.4 nm was found due to the twisted configuration of (*R*)-BINOL in **(*R*)-CuTAPBN-COF** (Figure 2a). HR-TEM revealed that each bulky particle consists of a series of crystalline flakes and a close analysis of the TEM-image shows that **(*R*)-CuTAPBN-COF** features grid structure (Figure 2b), which is well consistent with its structural modeling analysis. Notably, **(*R*)-CuTAPBN-COF** herein with other types of possible simulated space group gave the PXRD pattern that significantly deviated from the measured profile (Figure S1f).

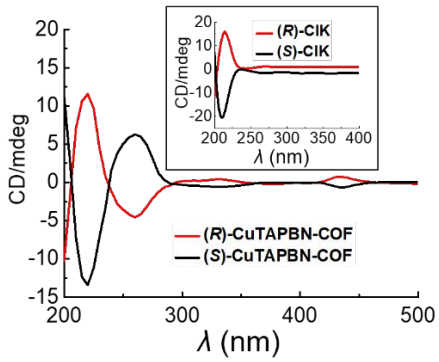

Figure 3. CD spectra showing that the pairs of **(*R*)-** and **(*S*)-CuTAPBN-COF**, and **(*R*)-** and **(*S*)-CIK** are mirror images of each other.

The N_2 absorption amount of **(*R*)-CuTAPBN-COF** at 77 K is 196.6 cm^3 g^{-1}, and the corresponding surface area on basis of BET model is 412.7 m^2 g^{-1} (Figure S1g). The pore-size distribution by nonlocal density functional theory (NLDFT) analysis indicates that it possesses the narrow pore diameter distribution centered at ~2.3 nm (Figure S1g inset). Owing to the existence of (*R*)-BINOL, **(*R*)-CuTAPBN-COF** is optically active and displays positive Cotton effect at 220 and 435 nm, and negative dichroic signal at 265 nm in its CD spectrum (Figure 3). In addition, the intense band at 419 nm, together with the weak bands between 539-572 nm, in its UV-vis spectrum demonstrates that the visible-light adsorption of Cu-TAPP is well retained in **(*R*)-CuTAPBN-COF** (Figure S1h). In addition, **(*R*)-CuTAPBN-COF** is stable against water, acid and base, which was verified by the measured PXRD patterns (Figure S1i).

The major advantage of **(*R*)-CuTAPBN-COF** is that the Lewis acid (Cu(II)),[15] chiral templating ((*R*)-BINOL) and photothermal conversion (Cu-TAPP) species are logically integrated on the HCCOF-platform, so its catalytic asymmetric synthesis of **(*S*)-CIK** via Strecker reaction under visible-light irradiation is highly expected.

The yield and enantiomeric excess (ee) for **(*R*)-CuTAPBN-COF**-catalyzed **(*S*)-CIK** synthesis, together with a series of control experiments, are displayed in Table 1 (entries 1-12). The catalytic reactions were performed under various conditions, including different solvents (entries 1-3), and catalysts with or without visible-light irradiation and heating (entries 4-12). The best result was obtained when the reaction was conducted in CH_3CN with **(*R*)-CuTAPBN-COF** (10 mg, 2.1 mol% Cu equiv) upon visible-light (λ = 420 nm) irradiation for 3h (entry 1). The desired **(*S*)-CIK** was

generated in 98% yield (TON = 46.7, TOF = 15.6 h^{-1}) with 94% ee. The measured reaction solution temperature was ~50°C under the given conditions, implying that the Cu-TAPP involved **(*R*)-CuTAPBN-COF** is an effective photothermal conversion material even at catalytic amount. Also, when the reaction was performed in CH_3CN with a lower catalyst loading (1.0 mol% Cu), the product was generated in lower 90% yield (92% ee) (entry 4). However, more catalyst loading (3.0 mol% Cu) did not afford higher yield (98%) and ee (95%) (entry 5). Notably, when the reaction was performed at 50°C in dark, **(*S*)-CIK** was obtained in 98% yield with 92% ee (entry 6). Furthermore, no product was detected once the reaction was conducted in the dark at room temperature within 3 h (entry 7). All these results unambiguously demonstrated that this HCCOF-promoted reaction herein is a thermally-driven reaction.[15] In the cases of copper-free **(*R*)-TAPBN-COF** (entries 8 and 9), only modest yields (17 and 18%) but with high enantioselectivity (93 and 95% ee) were observed under irradiation or heating condition, implying that the HCCOF-framework and the embedded Cu(II) are separately responsible for the chiral confinement effect and catalytic function, which was further supported by the cases of Cu-TAPP monomer (entry 10), $Cu(OAc)_2$ (entry 11) and the mixture of Cu-TAPP and (*R*)-BNOL (molar ratio of 1:2) (entry 12). Therefore, the confined environment, together with the active metal catalytic center, might afford the suitable compromise in enantioselectivity and yield for the chiral *α*-aminonitrile formation under elevated temperature.[16]

What's particularly intriguing is that the reaction could effectively proceed even under the natural sunlight irradiation (reaction solution temperature, ~47°C), and **(*S*)-CIK** was obtained in 70% yield with 92% ee within 3h (Table 1, entry 13). This provides a strong fundament for the future development of HCCOF-based and solar-powered endothermic asymmetric catalysis.

The subtle chiral confinement of **(*R*)-CuTAPBN-COF** was explored by preliminary molecular modeling studies. The calculations show that the initially formed iminium intermediate is restrained in the HCCOF pore by multiple C-H···X (X = F and O) H-bonds, and only the iminium with conformation tending to **(*S*)-CIK** can form the energy-favorable host-guest system (Figure S3), which allows the subsequent nucleophilic addition of CN^- to the carbonium ion of iminium along the pathway being lowered in energy and steric hindrance, consequently, generating the **(*S*)-CIK** with high optical purity.

In contrast, when the reaction was performed with **(*S*)-CuTAPBN-COF** (Figure S4 and Table S2), **(*R*)-CIK** was correspondingly obtained in 97% yield with 93% ee under the same conditions (Figure 3 and Figure S5). This suggests that we can consciously control the product enantioselectivity by finely tuning the HCCOF chirality, consequently achieving enantiopure product purposefully. Of note, the catalytic center and the chirality control herein are not on the same molecular entity, resembling what is happening in an enzyme pocket.

Table 1. Optimization of (*R*)-CuTAPBN-COF-Catalyzed Synthesis of (*S*)-CIK via Strecker Reaction[a]

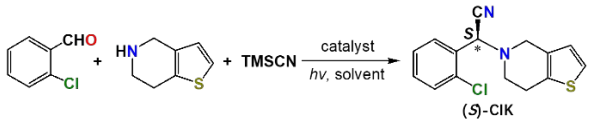

EN	catalyst	solvent	T (°C)/*hv*	yield (ee) %[b]
1	**(*R*)-CuTAPBN-COF** (2.1 mol Cu %)	CH_3CN	r.t./*hv*	98 (94)
2	**(*R*)-CuTAPBN-COF** (2.1 mol Cu %)	PhMe	r.t./*hv*	63 (90)
3	**(*R*)-CuTAPBN-COF** (2.1 mol Cu %)	EtOH	r.t./*hv*	45 (87)
4	**(*R*)-CuTAPBN-COF** (1.0 mol Cu %)	CH_3CN	r.t./*hv*	90 (92)
5	**(*R*)-CuTAPBN-COF** (3.0 mol Cu %)	CH_3CN	r.t./*hv*	98 (95)
6	**(*R*)-CuTAPBN-COF** (2.1 mol Cu %)	CH_3CN	50°C/dark	98 (92)
7	**(*R*)-CuTAPBN-COF** (2.1 mol Cu %)	CH_3CN	r.t./dark	- (-)
8	**(*R*)-TAPBN-COF** (2.1 mol %)	CH_3CN	r.t./*hv*	17 (95)
9	**(*R*)-TAPBN-COF** (2.1 mol %)	CH_3CN	50°C/dark	18 (93)
10	Cu-TAPP monomer (2.1 mol %)	CH_3CN	r.t./*hv*	81 (-)
11	$Cu(OAc)_2$ (2.1 mol Cu %)	CH_3CN	r.t./*hv*	85 (-)
12[c]	Cu-TAPP (2.1 mol Cu %) and (*R*)-BNOL	CH_3CN	r.t./*hv*	94(32)
13	**(*R*)-CuTAPBN-COF** (2.1 mol Cu %)	CH_3CN	r.t./sunlight	70 (92)

[a] Reaction conditions: catalyst, 2-chlorobenzaldehyde (56 *μ*L, 0.5 mmol), 4,5,6,7-tetrahydrothieno[3,2-c]pyridine (59 *μ*L, 0.5 mmol), trimethylsilyl cyanide (70 *μ*L, 0.55 mmol), CH_3CN (1.5 mL), 300 W xenon with a power density of 2.5 W cm^{-2} (λ = 420 nm), 3h, in air. [b] Product structure was determined by ^1H NMR and MS spectra (Figures S2a-b), yield was determined by the GC on HP-5 column, and ee was determined by HPLC with a Chiralcel OD-H column (90 : 10 = *n*-hexane : isopropanol, 0.8 mL min^{-1}, 247 nm) (Figure S2c). [c] Mixture of Cu-TAPP (2.1 mol Cu %) and (*R*)-BNOL with a molar ratio of 1:2.

To further evaluate the photothermal conversion of **(*R*)-CuTAPBN-COF**, the visible-light induced temperature increase (ΔT) was examined. When the reaction system of CH_3CN (1.5 mL)-HCCOF (10 mg) was irradiated with visible-light (λ = 420 nm, 2.5 W cm^{-2}) for 18 min., a significant temperature increase of 25°C was observed (Figure 4). As it is known, the paramagnetic metal ions inserted porphyrins can drastically decrease their excited-state lifetimes, thus funneling excited states into nonradiative decay pathways and quenching the porphyrin photochemistry intramolecularly, thereby causing the nonfluorescent **(*R*)-CuTAPBN-COF** to completely act in the photothermal mode, regardless of the state of the supramolecular system.[17-19] As a result, we concluded that the metalloporphyrin and chiral BIONL involved HCCOF herein is a multifunctional asymmetric catalytic material that is endowed with catalysis, chiral templating, and photothermal conversion functionalities.

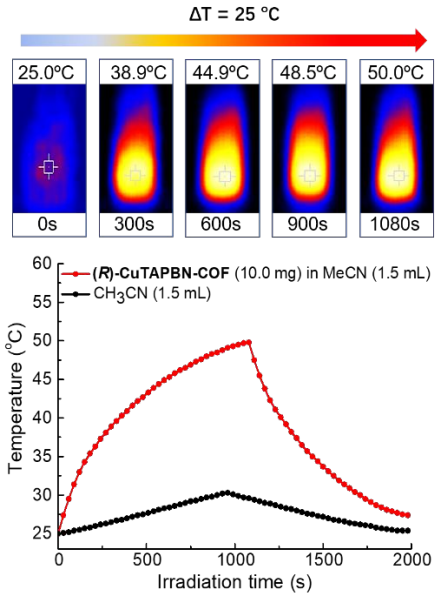

Figure 4. Photothermal behavior of **(*R*)-CuTAPBN-COF** (10 mg) in CH_3CN (1.5 mL).

The hot leaching test verified that **(*R*)-CuTAPBN-COF** is a typical heterogeneous catalyst (Figure S6), as such, it could be reused, and its catalytic yield was even up to 95% with 91% ee after five catalytic runs without loss of its structural integrity and crystallinity (Figure S6). Encouraged by the viability of the **(*R*)-CuTAPBN-COF**-catalyzed **(*S*)-CIK** synthesis, we then designed a model continuous flow-through setup for its gram-scale preparation.[20-23] This would allow overcoming the issues associated with batch operation in practical drug and drug intermediate production. Much to our delight, the asymmetric Strecker reaction by continuous flow-through operation proceeded smoothly under visible-light irradiation and gave a 90% yield (1.29 g) with 93% ee for **(*S*)-CIK** in 8h (Figure S7).

The generality of **(*R*)-CuTAPBN-COF**-catalyzed Strecker reaction was supported by utilizing various substrates (Figures S8-S9). The different aldehydes and secondary amines provided good-to-excellent yields with excellent ee values except those large-sized substrates, implying that the Strecker reaction herein is an internal surface catalytic process.

In summary, the concept of HCCOF-based multifunctional integration would allow this enantioselective synthesis to be applied more broadly to various other substrates for chiral drug discovery and preparation in a green and facile way.

ASSOCIATED CONTENT

Supporting Information. Instruments and methods; synthesis and additional characterization of **(*R*)-** and **(*S*)-CuTAPBN-COF**; catalytic products characterization; Continuous flow-through operation; molecular modeling studies; crystallographic information for COFs (PDF). This material is available free of charge via the Internet at http://pubs.acs.org.

AUTHOR INFORMATION

Corresponding Author

Gong-Jun Chen − College of Chemistry, Chemical Engineering and Materials Science, Collaborative Innovation Center of Functionalized Probes for Chemical Imaging in Universities of Shandong, Key Laboratory of Molecular and Nano Probes, Ministry of Education, Shandong Normal University, Jinan 250014, P. R. China; Email: gongjchen@126.com

Yu-Bin Dong − College of Chemistry, Chemical Engineering and Materials Science, Collaborative Innovation Center of Functionalized Probes for Chemical Imaging in Universities of Shandong, Key Laboratory of Molecular and Nano Probes, Ministry of Education, Shandong Normal University, Jinan 250014, P. R. China; orcid.org/0000-0002-9698-8863; Email: yubindong@sdnu.edu.cn

Authors

Hui-Chao Ma − College of Chemistry, Chemical Engineering and Materials Science, -Collaborative Innovation Center of Functionalized Probes for Chemical Imaging in Universities of Shandong, Key Laboratory of Molecular and Nano Probes, Ministry of Education, Shandong Normal University, Jinan 250014, P. R. China

Fang Huang − College of Chemistry, Chemical Engineering and Materials Science, Collaborative Innovation Center of Functionalized Probes for Chemical Imaging in Universities of Shandong, Key Laboratory of Molecular and Nano Probes, Ministry of Education, Shandong Normal University, Jinan 250014, P. R. China

Notes

The authors declare no competing financial interest.

ACKNOWLEDGMENT

We are grateful for financial support from NSFC (Grant Nos. 21971153 and 21671122), Chang-Jiang Scholars Program of China, Taishan Scholars Construction Project of Shandong Province, and Shandong Provincial Natural Science Foundation (No. ZR2018MB005).

REFERENCES

(1) Fabro, S.; Smith, R.; Williams, R. Toxicity and teratogenicity of optical isomers of thalidomide. *Nature* **1967**, *215*, 296.

(2) Gawley, R, E.; Aubé, J. Principles of asymmetric synthesis, Book·2nd Edition·2012.

(3) Morris, R., Bu, X. Induction of chiral porous solids containing only achiral building blocks. *Nature Chem*. **2010**, *2*, 353-361.

(4) Farina, V.; Reeves, J. T.; Senanayake, C. H.; Song, J. J. Asymmetric synthesis of active pharmaceutical ingredients. *Chem. Rev*. **2006**, *106*, 2734-2793.

(5) Saeed, A.; Shahzad, D.; Faisal, M.; Larik F. A.; El-Seedi, H. R.; Channar, P. A. Developments in the synthesis of the antiplatelet and antithrombotic drug (*S*)-clopidogrel. *Chirality* **2017**, *29*, 684-707.

(6) Casida, J. E. Why prodrugs and propesticides succeed. *Chem. Res. Toxicol*. **2107**, *30*, 1117-1126.

(7) Carpenter, J. S.; Rosenman, M. B.; Knisely, M. R.; Decker, B. S.; Levy, K. D.; Flockhart, D. A. Pharmacogenomically actionable medications in a safety net health care system. *SAGE Open Medicine* **2016**, *4*, 1-8.

(8) Gardell, S. J. Ticlopidine and clopidogrel: antithrombotic agents that block ADP-mediated platelet activation. *Perspect. Drug Discov*. **1994**, *1*, 521-526.

(9) Sadhukhan, A.; Saravanan, S.; Khan, N. H.; Kureshy, R. I.; Abdi, S. H. R.; Bajaj, H. C. Modified Asymmetric Strecker Reaction of Aldehyde with Secondary Amine: A Protocol for the Synthesis of

S−Clopidogrel (An Antiplatelet Agent). *J. Org. Chem.* **2012**, *77*, 7076-7080.

(10) Campos, K. R.; Coleman, P. J.; Alvarez, J. C.; Dreher, S. D.; Garbaccio, R. M.; Terrett, N. K.; Tillyer, R. D.; Truppo, M. D.; Parmee, E. R. The importance of synthetic chemistry in the pharmaceutical industry. *Science* **2019**, *363*, eaat0805.

(11) Côté, A. P.; Benin, A. I.; Ockwig, N. W.; O'Keeffe, M.; Matzger, A. J.; Yaghi, O. M. Porous, Crystalline, Covalent Organic Frameworks. *Science* **2005**, *310*, 1166-1170.

(12) The recent developments in HCCOF-based asymmetric catalysis are summarized in the minireview article: Ma, H.-C., Zou, J., Li, X.-T., Chen, G.-J, Dong, Y.-B. Homochiral Covalent Organic Frameworks for Asymmetric Catalysis. *Chem-Eur J.* **2020**, doi:10.1002/chem.202001006.

(13) Gröger, H. Catalytic enantioselective Strecker reactions and analogous syntheses. *Chem. Rev.* **2003**, *103*, 2795-2827.

(14) Ishitani, H.; Komiyama, S.; Hasegawa, Y.; Kobayashi, S. Catalytic Asymmetric Strecker Synthesis. Preparation of Enantiomerically Pure R-Amino Acid Derivatives from Aldimines and Tributyltin Cyanide or Achiral Aldehydes, Amines, and Hydrogen Cyanide Using a Chiral Zirconium Catalyst. *J. Am. Chem. Soc.* **2000**, *122*, 762-766.

(15) Hou, Y.-L.; Sun, R. W.-Y.; Zhou, X.-P.; Wang, J.-H.; Li, D. A copper(I)/copper(II)–salen coordination polymer as a bimetallic catalyst for three-component Strecker reactions and degradation of organic dyes. *Chem. Commun*. **2014**, *50*, 2295-2297.

(16) Ma, H.-C.; Zhao, C.-C.; Chen, G-J.; Dong, Y.-B. Photothermal conversion triggered thermal asymmetric catalysis within metal nanoparticles loaded homochiral covalent organic framework. *Nat Commun.* **2019**, *10*, 3368.

(17) Harriman, A. Luminescence of porphyrins and metalloporphyrins. *J. Chem. Soc. Faraday Trans.* **1980**, *176*, 1978-1985.

(18) Harriman, A. Luminescence of porphyrins and metalloporphyrins. *J. Chem. Soc Faraday Trans.* **1981**, *277*, 1281-1291.

(19) MacDonald, T. D.; Liu, T. W.; Zheng, G. An MRI-sensitive, non-photobleachable porphysome photothermal agent. *Angew. Chem., Int. Ed*. **2014**, *53*, 6956-6959.

(20) Li, F.; Ding, L.-G.; Yao, B.-J.; Huang, N.; Li, J.-T.; Fu, Q.-J.; Dong, Y.-B. Pd loaded and covalent-organic framework involved chitosan aerogels and their application for continuous flow-through aqueous CB decontamination. *J. Mater. Chem. A* **2018**, *6*, 11140-11146.

(21) Yao, B-J.; Li, J.-T.; Huang, N.; Kan, J.-L.; Qiao, L.; Ding, L.-G.; Li, F.; Dong, Y.-B. Pd NP-Loaded and Covalently Cross-Linked COF Membrane Microreactor for Aqueous CBs Dechlorination at Room Temperature. *ACS Appl. Mater. Interfaces* **2018**, *10*, 20448−20457.

(22) Ding, L.-G.; Yao, B.-J.; Li, F.; Shi, S.-C.; Huang, N.; Yin, H.-B.; Guan, Q.; Dong, Y.-B. Ionic liquid-decorated COF and its covalent composite aerogel for selective CO_2 adsorption and catalytic conversion. *J. Mater. Chem. A* **2019**, *7*, 4689–469.

(23) Wang, J.-C.; Liu, C.-X.; Kan, X.; Wu, X.-W.; Kan J.-L.; Dong, Y.-B. Pd@COF-QA: a phase transfer composite catalyst for aqueous Suzuki–Miyaura coupling reaction. *Green Chem.* **2020**, *22*, 1150-1155.

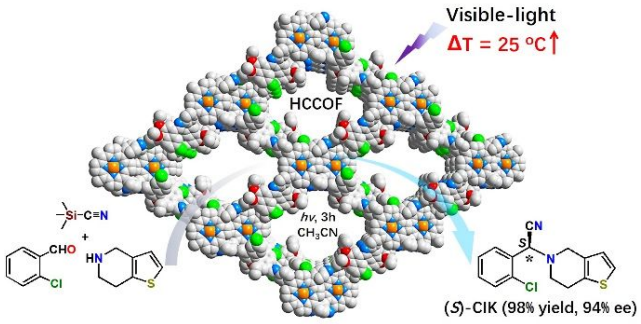

Table of Contents artwork